Study of $B_c^* \to \psi(1S,2S)P$, $\eta_c(1S,2S)P$ weak decays

Junfeng Sun,[1] Yueling Yang,[1] Na Wang,[1] Jinshu Huang,[2] and Qin Chang[1]

[1]*Institute of Particle and Nuclear Physics, Henan Normal University, Xinxiang 453007, China*

[2]*College of Physics and Electronic Engineering, Nanyang Normal University, Nanyang 473061, China*

arXiv:1703.00155v1 [hep-ph] 1 Mar 2017

Abstract

Motivated by the potential prospects of the B_c^* meson samples at hadron colliders, the bottom-changing $B_c^* \to \psi(1S,2S)P$, $\eta_c(1S,2S)P$ weak decays are first studied with the perturbative QCD approach, where $P = \pi$ and K. It is found that branching ratio of the CKM-favored $B_c^* \to J/\psi\pi$ decay is about $\sim \mathcal{O}(10^{-8})$, which might be measurable at the future LHC experiments.

I. INTRODUCTION

The B_c^* meson consists of two heavy quarks with different flavor numbers, i.e., $\bar{b}c$ ($b\bar{c}$) for the B_c^{*+} (B_c^{*-}) meson. The B_c^* meson is a spin-triplet ground state ($n^{2s+1}L_J = 1^3S_1$). The B_c^* meson lies below the BD meson pair threshold. What is more, the mass difference $m_{B_c^*} - m_{B_c} \simeq 50$ MeV [1] is far less than the mass of pion. So, the B_c^* meson decays via the strong interaction are completely forbidden. However, the B_c^* meson decays through the electromagnetic and weak interactions are allowable within the standard model of elementary particles. The dominant magnetic dipole (M1) transition, $B_c^* \to B_c\gamma$, is strongly suppressed by the compact phase spaces, which results in a lifetime $\tau_{B_c^*} \sim \mathcal{O}(10^{-18}\,\mathrm{s})$ [2]. Besides, the B_c^* meson carries explicitly nonzero bottom and charm quantum numbers ($B = C = \pm 1$). Hence, the B_c^* meson can decay by means of the flavor-changing weak transitions.

The B_c^* meson weak decays, similar to the B_c meson weak decays [3–9], can be divided into three classes: (1) the b quark decay with the c quark as a spectator, (2) the c quark decay with the b quark as a spectator, and (3) the b and c quarks annihilation into a virtual $W^{\pm}$ boson. The B_c^* meson has a large mass. In addition, both constituent quarks of the B_c^* meson can decay individually. Therefore, the B_c^* meson has abundant weak decay channels. However, the B_c^* meson weak decays have received much less attention in the past. There is no experimental measurement report [10] and few theoretical investigations concerned with the B_c^* weak decay. Fortunately, with the high luminosity and large production cross section of the B_c^* meson [11–14] at the running LHC, a huge amount of the B_c^* meson data samples would be accumulated. Some of the B_c^* meson weak decays might be explored in the future. The B_c^* meson provides another laboratory to study the heavy flavor weak decay.

In this paper, we will study the nonleptonic $B_c^* \to \psi(1S, 2S)P$, $\eta_c(1S, 2S)P$ decays with the perturbative QCD (pQCD) approach [15–17], where $P = \pi$ and K. Our motivations are as follows. Firstly, due to the development of experimental instruments and technology, final states of the charmonium and the charged pion and/or kaon are easy to identify experimentally. With the advancement of high energy hadron collider experiments, the $B_c \to \psi(1S, 2S)P$ decays have been observed [10, 18–23]. Due to the production cross section $\sigma(B_c^*) \gtrsim \sigma(B_c)$ in hadron collisions [11–14], hopefully, it is anticipated that the $B_c^* \to \psi(1S, 2S)P$, $\eta_c(1S, 2S)P$ decays might be observed experimentally in the future. A theoretical study on the $B_c^* \to \psi(1S, 2S)P$, $\eta_c(1S, 2S)P$ decays is necessary to provide the future

experimental investigation with an immediate reference. Secondly, due to the relations of $\sigma(B_c^*) \gtrsim \sigma(B_c)$ and $m_{B_c^*} \simeq m_{B_c}$ [1], one possible background for the B_c meson decays might come from the B_c^* meson decays into the same final states. Hence, the study of the $B_c^* \to \psi(1S,2S)P$, $\eta_c(1S,2S)P$ decays will provide some useful information for the experimental analysis on the $B_c \to \psi(1S,2S)P$, $\eta_c(1S,2S)P$ decays. Thirdly, as it is well known, the Cabibbo-Kobayashi-Maskawa (CKM) matrix element $|V_{cb}|$ could be determined from the semileptonic decays of the B meson to the $D^{(*)}$ meson. However, there exists a more than $3.0\,\sigma$ discrepancy between the values from exclusive and inclusive determinations[a] [10]. The $B_c^{(*)} \to \psi(1S,2S)P$, $\eta_c(1S,2S)P$ decays are induced actually by the $b \to c$ (or $\bar{b} \to \bar{c}$) transition at the quark level. The weak interaction coupling and the decay amplitudes are proportional to the CKM matrix element $|V_{cb}|$ [see Eq.(1) or Eqs.(37)-(39)]. Hence, the $B_c^{(*)} \to \psi(1S,2S)P$, $\eta_c(1S,2S)P$ decays, together with nonleptonic $\overline{B} \to D^{(*)}X$ decays and semileptonic $\overline{B} \to D^{(*)}\ell\bar{\nu}$ decays, are expected to give more stringent constraints on the CKM matrix element $|V_{cb}|$, other parameters extracted from the B meson decays, and contributions from possible new physics. Fourthly, owing to the same dynamical mechanism of the bottom quark decay, many phenomenological models used for the B meson decays could, in principle, be generalized and applied to the B_c^* meson weak decays. The practical applicability and reliability of the pQCD approach can be reevaluated with the $B_c^* \to \psi(1S,2S)P$, $\eta_c(1S,2S)P$ decays. Further, the $B_c^* \to \psi(1S,2S)P$, $\eta_c(1S,2S)P$ decays provide an opportunity to study polarization effects involved in the vector meson decays.

This paper is organized as follows. The theoretical framework and decay amplitudes with the pQCD approach are presented in Section II. Section III is devoted to the numerical results and discussion. The last section is a summary.

II. THEORETICAL FRAMEWORK

A. The effective Hamiltonian

By means of the operator product expansion and the renormalization group (RG) method, the effective Hamiltonian responsible for the $B_c^* \to \psi(1S,2S)P$, $\eta_c(1S,2S)P$ weak decays

[a] The values of the CKM element $|V_{cb}|$ obtained from inclusive and exclusive determinations are $|V_{cb}| = (42.2\pm0.8)\times10^{-3}$ and $(39.2\pm0.7)\times10^{-3}$, respectively [10].

is expressed in terms of four-quark operators with the process-independent couplings of the Wilson coefficients C_i [24],

$$\mathcal{H}_{\rm eff} \;=\; \frac{G_F}{\sqrt{2}} \sum_{q=d,s} V_{cb}^* V_{uq} \Big\{ C_1 \, (\bar{b}_\alpha \, c_\alpha)_{V-A} \, (\bar{u}_\beta \, q_\beta)_{V-A} + C_2 \, (\bar{b}_\alpha \, c_\beta)_{V-A} \, (\bar{u}_\beta \, q_\alpha)_{V-A} \Big\} + \text{h.c.}, \quad (1)$$

where the Fermi coupling constant $G_F \simeq 1.166 \times 10^{-5}\,\text{GeV}^{-2}$ [10]; current operator $(\bar{q}_1 \, q_2)_{V-A}$ $= \bar{q}_1 \, \gamma_\mu (1-\gamma_5) \, q_2$; α and β are color indices. The CKM factor $V_{cb}^* V_{uq}$ can be written in terms of the Wolfenstein parameters [10], i.e.,

$$V_{cb}^* V_{ud} \;=\; A\,\lambda^2 - \frac{1}{2}\,A\,\lambda^4 - \frac{1}{8}\,A\,\lambda^6 + \mathcal{O}(\lambda^8), \qquad \text{for } P \,=\, \pi; \quad (2)$$

$$V_{cb}^* V_{us} \;=\; A\,\lambda^3 + \mathcal{O}(\lambda^8), \qquad \text{for } P \,=\, K. \quad (3)$$

The auxiliary parameter μ separates the physical contributions into two parts. The hard contributions above the scale μ are summarized into the Wilson coefficients $C_i(\mu)$. Due to the properties of asymptotic freedom of QCD forces, the Wilson coefficients are, in principle, computable order by order with the RG equation improved perturbation theory as long as the scale μ is not too small [24]. The physical contributions below the scale μ are included in the hadronic matrix elements (HME) where the local four-quark operators are sandwiched between initial and final states. The participating hadrons are bounds states of partons. With the participation of the strong interaction in the transition from quarks to hadrons, especially, the presence of long-distance QCD effects and the entanglement of nonperturbative and perturbative contributions, how to properly evaluate HME is one of major tasks for a serious phenomenology of weak decays of heavy flavor hadrons.

B. Hadronic matrix elements

Phenomenologically, one has to turn to some approximation or assumption for the HME calculation. The Lepage-Brodsky approach [25] is usually applied to a hard scattering process, where a hadron transition matrix element is generally written as a convolution integral of hadron wave functions reflecting the nonperturbative contributions and hard scattering amplitudes containing perturbative contributions. In order to wipe out the endpoint singularities appearing in the collinear approximation [26–28] and suppress the soft contributions, as it is argued with the pQCD approach [15–17], the transverse momentum k_T of valence quarks should be retained and Sudakov factor e^{-S} should be introduced for each of the wave

functions. Finally, the B_c^* weak decay amplitude can be expressed as a multidimensional integral of many parts [16, 17], including the hard effects enclosed by the Wilson coefficients C_i, the heavy quark decay amplitudes $\mathcal{H}$, and the universal wave functions Φ,

$$\mathcal{A} \sim \sum_i \int \prod_j dk_j \, C_i(t) \, \mathcal{H}_i(t, k_j) \, \Phi_j(k_j) \, e^{-S_j}, \tag{4}$$

where t is a typical scale, k_j is the momentum of a valence quark.

C. Kinematic variables

In the rest frame of the B_c^* meson, the light-cone kinematic variables are defined as follows.

$$p_1 = \frac{m_1}{\sqrt{2}}(1, 1, 0), \tag{5}$$

$$p_2 = (p_2^+, p_2^-, 0), \tag{6}$$

$$p_3 = (p_3^-, p_3^+, 0), \tag{7}$$

$$k_i = x_i \, p_i + (0, 0, \vec{k}_{iT}), \tag{8}$$

$$p_i^\pm = (E_i \pm p)/\sqrt{2}, \tag{9}$$

$$\epsilon_1^\parallel = \frac{1}{\sqrt{2}}(-1, 1, 0), \tag{10}$$

$$\epsilon_2^\parallel = \frac{1}{m_2}(p_2^+, -p_2^-, 0), \tag{11}$$

$$\epsilon_{1,2}^\perp = (0, 0, \vec{1}), \tag{12}$$

$$s = 2 \, p_2 \cdot p_3, \tag{13}$$

$$t = 2 \, p_1 \cdot p_2 = 2 \, m_1 \, E_2, \tag{14}$$

$$u = 2 \, p_1 \cdot p_3 = 2 \, m_1 \, E_3, \tag{15}$$

$$s \, t + s \, u - t \, u = 4 \, m_1^2 \, p^2, \tag{16}$$

where for variables including the momentum p_i, mass m_i, energy E_i, and longitudinal (transverse) polarization vector $\epsilon_i^\parallel$ ($\epsilon_i^\perp$), the subscript $i = 1, 2, 3$ stands for the B_c^* meson, charmonium ψ (η_c), and pseudoscalar meson P, respectively; k_i is the momentum of a valence quark; x_i and k_{iT} are the longitudinal momentum fraction and transverse momentum, respectively; p is the center-of-mass momentum of final states; s, t and u are the Lorentz invariant parameters. The kinematic variables are displayed in Fig.2(a).

D. Wave functions

It is seen from Eq.(4) that wave functions are essential input parameters with the pQCD approach. And in general, wave functions are universal, i.e., process independent. Following the notations in Refs.[29, 30], wave functions of participating mesons are defined as

$$\langle 0|\bar{b}_i(0)c_j(z)|B_c^*(p,\epsilon^{\parallel})\rangle \;=\; \frac{f_{B_c^*}}{4}\int d^4k\, e^{-ik\cdot z}\Big\{\not{\epsilon}^{\parallel}\Big[m_{B_c^*}\,\Phi^v_{B_c^*}(k)-\not{p}\,\Phi^t_{B_c^*}(k)\Big]\Big\}_{ji}, \tag{17}$$

$$\langle 0|\bar{b}_i(0)c_j(z)|B_c^*(p,\epsilon^{\perp})\rangle \;=\; \frac{f_{B_c^*}}{4}\int d^4k\, e^{-ik\cdot z}\Big\{\not{\epsilon}^{\perp}\Big[m_{B_c^*}\,\Phi^V_{B_c^*}(k)-\not{p}\,\Phi^T_{B_c^*}(k)\Big]\Big\}_{ji}, \tag{18}$$

$$\langle \psi(p,\epsilon^{\parallel})|c_i(0)\bar{c}_j(z)|0\rangle \;=\; \frac{f_{\psi}}{4}\int d^4k\, e^{+ik\cdot z}\Big\{\not{\epsilon}^{\parallel}\Big[m_{\psi}\,\Phi^v_{\psi}(k)+\not{p}\,\Phi^t_{\psi}(k)\Big]\Big\}_{ji}, \tag{19}$$

$$\langle \psi(p,\epsilon^{\perp})|c_i(0)\bar{c}_j(z)|0\rangle \;=\; \frac{f_{\psi}}{4}\int d^4k\, e^{+ik\cdot z}\Big\{\not{\epsilon}^{\perp}\Big[m_{\psi}\,\Phi^V_{\psi}(k)+\not{p}\,\Phi^T_{\psi}(k)\Big]\Big\}_{ji}, \tag{20}$$

$$\langle \eta_c(p)|c_i(0)\bar{c}_j(z)|0\rangle \;=\; \frac{i\,f_{\eta_c}}{4}\int d^4k\, e^{+ik\cdot z}\Big\{\gamma_5\Big[\not{p}\,\Phi^a_{\eta_c}(k)+m_{\eta_c}\,\Phi^p_{\eta_c}(k)\Big]\Big\}_{ji}, \tag{21}$$

$$\langle P(p)|\bar{u}_i(0)q_j(z)|0\rangle \;=\; \frac{i\,f_P}{4}\int d^4k\, e^{+ik\cdot z}\Big\{\gamma_5\Big[\not{p}\,\Phi^a_P(k)+\mu_P\,\Phi^p_P(k)+\mu_P\,(\not{n}_+\not{n}_- -1)\,\Phi^t_P(k)\Big]\Big\}_{ji}, \tag{22}$$

where $f_{B_c^*}$, f_{ψ}, f_{η_c} and f_P are decay constants; wave functions of $\Phi^{v,T}$ and Φ^a are twist-2; $\Phi^{V,t}$ and $\Phi^{p,t}$ are twist-3; $\mu_P = m_3^2/(m_u+m_q)$ is the chiral parameter; n_+ and n_- are the positive and negative null vectors, respectively.

For the light pseudoscalar meson P, only the leading twist (twist-2) distribution amplitude (DA) $\phi_P^a(x)$ is involved in our calculation (see the Appendix). And the normalized DA $\phi_P^a(x)$ has the following general structure [30]:

$$\phi_P^a(x) \;=\; 6\,x\,\bar{x}\Big\{1+\sum_{n=1} a_n^P\, C_n^{3/2}(t)\Big\}, \tag{23}$$

where $\bar{x}=1-x$ and $t=x-\bar{x}$; the Gegenbauer moment a_n^P is a nonperturbative parameter. The Gegenbauer polynomials are expressed as:

$$C_1^{3/2}(t)=3\,t, \quad C_2^{3/2}(t)=\frac{3}{2}\,(5\,t^2-1), \quad \cdots \tag{24}$$

The B_c^* meson and charmonium ψ and η_c consist of two heavy flavors. The motion of the valence quarks in these mesons should be nearly nonrelativistic. Taking a similar treatment of the nonrelativistic heavy quarkonium system [31–34], DAs for the B_c^* meson and charmonium can be written as

$$\phi^{v,T}_{B_c^*}(x) = A\,x\,\bar{x}\exp\Big\{-\frac{\bar{x}\,m_c^2+x\,m_b^2}{8\,\omega_1^2\,x\,\bar{x}}\Big\}, \tag{25}$$

$$\phi^t_{B_c^*}(x) = B\,(\bar{x}-x)^2\exp\Big\{-\frac{\bar{x}\,m_c^2+x\,m_b^2}{8\,\omega_1^2\,x\,\bar{x}}\Big\}, \tag{26}$$

$$\phi^V_{B_c^*}(x) = C\,\big\{1+(\bar{x}-x)^2\big\}\exp\Big\{-\frac{\bar{x}\,m_c^2+x\,m_b^2}{8\,\omega_1^2\,x\,\bar{x}}\Big\}, \tag{27}$$

$$\phi^a_{\eta_c(1S)}(x) = \phi^{v,T}_{\psi(1S)}(x) = D\,x\,\bar{x}\exp\Big\{-\frac{m_c^2}{8\,\omega_2^2\,x\,\bar{x}}\Big\}, \tag{28}$$

$$\phi^t_{\psi(1S)}(x) = E\,(\bar{x}-x)^2\exp\Big\{-\frac{m_c^2}{8\,\omega_2^2\,x\,\bar{x}}\Big\}, \tag{29}$$

$$\phi^V_{\psi(1S)}(x) = F\,\big\{1+(\bar{x}-x)^2\big\}\exp\Big\{-\frac{m_c^2}{8\,\omega_2^2\,x\,\bar{x}}\Big\}, \tag{30}$$

$$\phi^p_{\eta_c(1S)}(x) = G\exp\Big\{-\frac{m_c^2}{8\,\omega_2^2\,x\,\bar{x}}\Big\}, \tag{31}$$

$$\phi^{v,t,V,T}_{\psi(2S)}(x) = H\,\phi^{v,t,V,T}_{\psi(1S)}(x)\,\Big\{1+\frac{m_c^2}{2\,\omega_2^2\,x\,\bar{x}}\Big\}, \tag{32}$$

$$\phi^{a,p}_{\eta_c(2S)}(x) = I\,\phi^{a,p}_{\eta_c(1S)}(x)\,\Big\{1+\frac{m_c^2}{2\,\omega_2^2\,x\,\bar{x}}\Big\}, \tag{33}$$

where parameter $\omega_i \simeq m_i\,\alpha_s(m_i)$ determines the average transverse momentum of valence quarks according to the power counting rules of nonrelativistic QCD effective theory [35–37]; parameters A, B, C, D, E, F, G, H, I in Eqs.(25-33) could be explicitly determined with the following normalization conditions,

$$\int_0^1 dx\,\phi^{v,t,V,T}_{B_c^*}(x) = 1, \tag{34}$$

$$\int_0^1 dx\,\phi^{v,t,V,T}_{\psi}(x) = 1, \tag{35}$$

$$\int_0^1 dx\,\phi^{a,p}_{\eta_c}(x) = 1. \tag{36}$$

The shape lines of the normalized DAs of participating mesons are illustrated in Fig.1. It is clearly seen from Fig.1 that (1) a broad peak appears at $x < 0.5$ region for DAs of the B_c^* meson. (2) The shape lines of DAs for the $\psi(1S,2S)$ and $\eta_c(1S,2S)$ mesons are symmetric versus x, which agree basically with the postulated scenario that patrons share momentum fractions according to their masses. (3) The differences between DAs of ϕ^a_π and ϕ^a_K arise from the flavor symmetry breaking effects representing by the Gegenbauer moment $a_1^K \neq 0$. (4) Owing to the exponential functions, the shape lines of DAs in Eqs.(25-33) fall quickly down to zero at endpoints x, $\bar{x} \to 0$. So the DAs of Eqs.(25-33) will give an effective cut for the soft contributions from the endpoints.

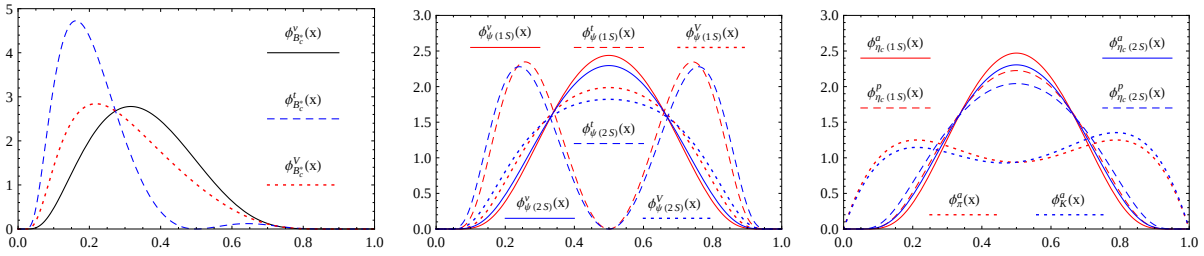

(a) (b) (c)

FIG. 1: The normalized distribution amplitudes of $\phi_{B_c^*}^{v,t,V}(x)$, $\phi_{\psi}^{v,t,V}(x)$, $\phi_{\eta_c}^{a,p}(x)$ and $\phi_{\pi,K}^{a}(x)$.

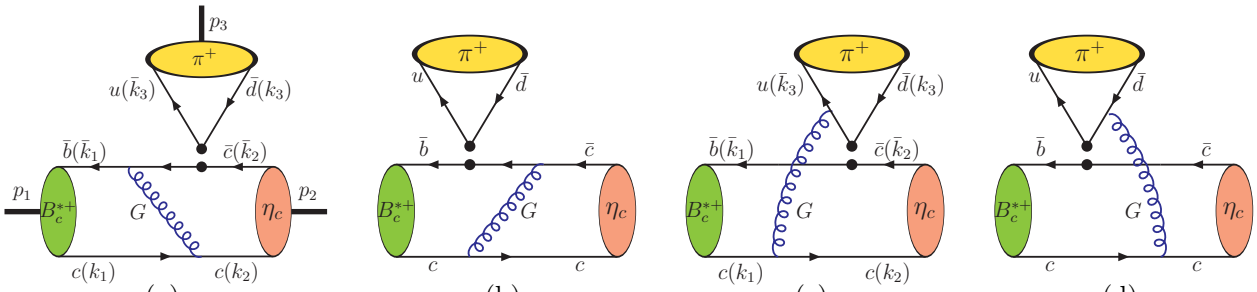

(a) (b) (c) (d)

FIG. 2: Feynman diagrams for the $B_c^{*+} \to \eta_c \pi^+$ decay, where (a,b) are factorizable emission topologies, (c,d) are nonfactorizable emission topologies.

E. Decay amplitudes

The Feynman diagrams for the $B_c^* \to \eta_c \pi$ decay are displayed in Fig.2, including factorizable topologies (a,b) where one gluon couples the B_c^* meson with the recoiled η_c meson, nonfactorizable topologies (c,d) where one gluon is exchanged between the spectator quark and the emitted π meson.

The Lorentz invariant amplitudes for the $B_c^* \to \psi P$, $\eta_c P$ decays are written as

$$\mathcal{A}(B_c^* \to \psi P) \;=\; i\,\mathcal{F}\,f_\psi \sum_i \left\{ \mathcal{A}_{i,L}(\epsilon^{\parallel}_{B_c^*}, \epsilon^{\parallel}_{\psi}) + \mathcal{A}_{i,N}\,(\epsilon^{\perp}_{B_c^*} \cdot \epsilon^{\perp}_{\psi}) + i\,\mathcal{A}_{i,T}\,\varepsilon_{\alpha\beta\mu\nu}\,p^{\alpha}_{B_c^*}\,p^{\beta}_{\psi}\,\epsilon^{\mu}_{B_c^*}\,\epsilon^{\nu}_{\psi} \right\}, \quad (37)$$

$$\mathcal{A}(B_c^* \to \eta_c P) \;=\; \mathcal{F}\,f_{\eta_c} \sum_i A_{i,P}, \quad (38)$$

$$\mathcal{F} \;=\; \frac{G_F}{\sqrt{2}}\,V_{cb}^*\,V_{uq}\,\frac{\pi\,C_F}{N_c}\,f_{B_c^*}\,f_P, \quad (39)$$

where the subscript i on $\mathcal{A}_{i,j}$ corresponds to one of the indices in Fig.2; the subscript j refers to different helicity amplitudes; and the expressions of building blocks $\mathcal{A}_{i,j}$ are collected in the Appendix. The helicity amplitudes for $B_c^* \to \psi P$ decays are defined as

$$\mathcal{M}_0 \;=\; -\mathcal{F} \sum_i \mathcal{A}_{i,L}(\epsilon^{\parallel}_{B_c^*}, \epsilon^{\parallel}_{\psi}), \quad (40)$$

$$\mathcal{M}_{\parallel} \;=\; \sqrt{2}\,\mathcal{F}\sum_i \mathcal{A}_{i,N}, \tag{41}$$

$$\mathcal{M}_{\perp} \;=\; \sqrt{2}\,\mathcal{F}\,m_{B_c^*}\,p\sum_i \mathcal{A}_{i,T}. \tag{42}$$

III. NUMERICAL RESULTS AND DISCUSSION

In the rest frame of the B_c^* meson, branching ratios for the $B_c^* \to \psi P$, $\eta_c P$ decays are defined as

$$\mathcal{B}r(B_c^*\to\psi P) \;=\; \frac{1}{24\pi}\,\frac{p}{m^2_{B_c^*}\Gamma_{B_c^*}}\left\{|\mathcal{M}_0|^2+|\mathcal{M}_{\parallel}|^2+|\mathcal{M}_{\perp}|^2\right\}, \tag{43}$$

$$\mathcal{B}r(B_c^*\to\eta_c P) \;=\; \frac{1}{24\pi}\,\frac{p}{m^2_{B_c^*}\Gamma_{B_c^*}}\,|\mathcal{A}(B_c^*\to\eta_c P)|^2, \tag{44}$$

where $\Gamma_{B_c^*}$ is the full width of the B_c^* meson.

TABLE I: The numerical values of input parameters.

CKM parameter[10]	$A = 0.811\pm0.026$,	$\lambda = 0.22506\pm0.00050$,
$m_{B_c^*} = 6332\pm9$ MeV[a] [1],	$m_{\psi(1S)} = 3096.900\pm0.006$ MeV [10],	$\Lambda^{(5)}_{\rm QCD} = 210\pm14$ MeV [10],
$m_b = 4.78\pm0.06$ GeV [10],	$m_{\psi(2S)} = 3686.097\pm0.025$ MeV [10],	$\Lambda^{(4)}_{\rm QCD} = 292\pm16$ MeV [10],
$m_c = 1.67\pm0.07$ GeV [10],	$m_{\eta_c(1S)} = 2983.4\pm0.5$ MeV [10],	$a_1^{\pi} = 0$ [30],
$f_{B_c^*} = 422\pm13$ MeV [38],	$m_{\eta_c(2S)} = 3639.2\pm1.2$ MeV [10],	a_2^{π} (1 GeV) $= 0.25\pm0.15$ [30],
$f_{\pi} = 130.2\pm1.7$ MeV [10],	$m_{\pi} = 139.57$ MeV [10],	a_1^{K} (1 GeV) $= 0.06\pm0.03$ [30],
$f_K = 155.6\pm0.4$ MeV [10],	$m_K = 493.677\pm0.016$ MeV [10],	a_2^{K} (1 GeV) $= 0.25\pm0.15$ [30],

[a]More predictions of the B_c^* meson mass with different models can be found in Table II of Ref.[39].

The numerical values of some input parameters are listed in Table I. If it is not specified explicitly, their central values will be used in the calculation.

The decay constant f_ψ is related with the branching ratio for the leptonic decay $\psi \to e^+e^-$ through the formula [40]

$$\mathcal{B}r(\psi\to e^+e^-) \;=\; \frac{4\,\pi\,Q_c^2\,\alpha^2_{\rm em}\,f_\psi^2}{3\,m_\psi\,\Gamma_\psi}, \tag{45}$$

where Q_c is the charge of the charm quark in unit of $|e|$; $\alpha_{\rm em}$ is the fine-structure constant of the electromagnetic interaction; Γ_ψ is full decay width of the ψ meson. From the available experimental data of both $\mathcal{B}r(\psi(1S)\to e^+e^-) = (5.971\pm0.032)\%$ and $\mathcal{B}r(\psi(2S)\to e^+e^-) =$

$(7.89\pm0.17)\times10^{-3}$ [10], one can obtain $f_{\psi(1S)} = (416.2\pm7.4)$ MeV and $f_{\psi(2S)} = (294.6\pm7.2)$ MeV, respectively. The decay constant f_{η_c} can be extracted from the branching ratio for the η_c meson decay into two photons using the formula [40]

$$\mathcal{B}r(\eta_c\to\gamma\gamma) \;=\; \frac{4\,\pi\,Q_c^4\,\alpha_{\rm em}^2\,f_{\eta_c}^2}{m_{\eta_c}\,\Gamma_{\eta_c}}. \tag{46}$$

With the up-to-date data of $\mathcal{B}r(\eta_c(1S)\to\gamma\gamma) = (1.59\pm0.13)\times10^{-4}$ and $\mathcal{B}r(\eta_c(2S)\to\gamma\gamma) = (1.9\pm1.3)\times10^{-4}$ [10], one can obtain $f_{\eta_c(1S)} = (337.7\pm18.2)$ MeV and $f_{\eta_c(2S)} = (243.1\pm127.4)$ MeV, respectively.

Besides, the full width of the B_c^* meson, $\Gamma_{B_c^*}$, is also an essential input parameter. Because the electromagnetic radiation process $B_c^* \to B_c\gamma$ dominates the B_c^* meson decay, an approximation $\Gamma_{B_c^*} \simeq \Gamma(B_c^*\to B_c\gamma)$ will be used here. However, unfortunately, the photon from the $B_c^* \to B_c\gamma$ process is not hard enough, so, it is fairly challenging to identify experimentally. The information on $\Gamma(B_c^*\to B_c\gamma)$ comes mainly from theoretical estimations. Theoretically, the partial decay width of the spin-flip M1 transition process has the expression [2],

$$\Gamma(B_c^*\to B_c\gamma) \;=\; \frac{4}{3}\,\alpha_{\rm em}\,k_\gamma^3\,\mu_h^2, \tag{47}$$

where k_γ is the photon momentum in the rest frame of the B_c^* meson; μ_h is the M1 moment of the B_c^* meson. There are plenty of theoretical predictions on $\Gamma(B_c^*\to B_c\gamma)$ with different approaches, such as various potential models [41–49]. However, because of the incomprehension about μ_h, these estimations suffer from large uncertainties, $\Gamma(B_c^*\to B_c\gamma) \simeq 20\sim80$ eV [41–49] (see the numbers in Tables 3 and 6 in Ref.[2]). To give a quantitative estimation, a ballpark guess $\Gamma_{B_c^*} \simeq (50\pm30)$ eV will be employed here for the moment, where an assumed uncertainty is given to be marginally consistent with previous results [41–49].

TABLE II: Branching ratios for the $B_c^* \to \psi P$, $\eta_c P$ decays, where the theoretical uncertainties come from scale $(1\pm0.1)t_i$, mass m_c and m_b, the CKM parameters, and $\Gamma_{B_c^*}$, respectively.

final states	branching ratio	final states	branching ratio
$\psi(1S)\pi$	$(9.16^{+0.98+1.13+0.68+13.74}_{-0.45-0.25-0.65-\ 3.43})\times10^{-8}$	$\psi(2S)\pi$	$(3.21^{+0.39+0.26+0.24+4.81}_{-0.17-0.32-0.23-1.20})\times10^{-8}$
$\eta_c(1S)\pi$	$(2.22^{+0.28+0.06+0.16+3.32}_{-0.12-0.08-0.16-0.83})\times10^{-8}$	$\eta_c(2S)\pi$	$(4.59^{+0.57+0.63+0.34+6.88}_{-0.25-0.86-0.33-1.72})\times10^{-9}$
$\psi(1S)K$	$(7.28^{+0.80+0.57+0.58+10.93}_{-0.36-0.46-0.55-\ 2.73})\times10^{-9}$	$\psi(2S)K$	$(2.37^{+0.28+0.28+0.19+3.55}_{-0.13-0.18-0.18-0.89})\times10^{-9}$
$\eta_c(1S)K$	$(1.67^{+0.21+0.04+0.13+2.51}_{-0.09-0.07-0.13-0.63})\times10^{-9}$	$\eta_c(2S)K$	$(3.42^{+0.43+0.45+0.27+5.12}_{-0.19-0.66-0.26-1.28})\times10^{-10}$

Our numerical results are presented in Table II, where the uncertainties come from the typical scale $(1\pm0.1)t_i$, mass m_c and m_b, the CKM parameters, and the decay width $\Gamma_{B_c^*}$, respectively. The followings are some comments.

(1) Because of the hierarchical relations between the CKM matrix elements $|V_{ud}| > |V_{us}|$, branching ratios for the $B_c^* \to \psi K$, $\eta_c K$ decays are generally an order of magnitude less than those for the $B_c^* \to \psi\pi$, $\eta_c\pi$ decays with the same charmonium in the final states, i.e.,

$$\mathcal{B}r(B_c^*\to\psi\pi) > \mathcal{B}r(B_c^*\to\psi K), \tag{48}$$

$$\mathcal{B}r(B_c^*\to\eta_c\pi) > \mathcal{B}r(B_c^*\to\eta_c K). \tag{49}$$

Due to the hierarchical relations between decay constants $f_{\psi(1S)} > f_{\psi(2S)}$ and $f_{\eta_c(1S)} > f_{\eta_c(2S)}$, along with relatively compact phase spaces for final $\psi(2S)P$, $\eta_c(2S)P$ states with respect to those for the $\psi(1S)P$, $\eta_c(1S)P$ states, there are some hierarchical relations, i.e.,

$$\mathcal{B}r(B_c^*\to\psi(1S)P) > \mathcal{B}r(B_c^*\to\psi(2S)P), \tag{50}$$

$$\mathcal{B}r(B_c^*\to\eta_c(1S)P) > \mathcal{B}r(B_c^*\to\eta_c(2S)P), \tag{51}$$

for the same final pseudoscalar meson P.

In addition, due to the conservation of angular momentum, there are more wave amplitudes contributing to the $B_c^* \to \psi P$ decays than the only p-wave amplitudes contributing to the $B_c^* \to \eta_c P$ decays. So there are some hierarchical relations, i.e.,

$$\mathcal{B}r(B_c^*\to\psi(1S)P) > \mathcal{B}r(B_c^*\to\eta_c(1S)P), \tag{52}$$

$$\mathcal{B}r(B_c^*\to\psi(2S)P) > \mathcal{B}r(B_c^*\to\eta_c(2S)P), \tag{53}$$

for the same final pseudoscalar meson P.

(2) The branching ratios of the $B_c^* \to \psi P$, $\eta_c P$ decays are several orders of magnitude less than the branching ratios of the $B_c \to \psi P$, $\eta_c P$ decays [7, 8]. So, the possible influence from the B_c^* meson decays could be safely neglected when the $B_c \to \psi P$, $\eta_c P$ decays are studied experimentally. On the other hand, with the improvement of detection ability and analytical techniques, rare B decay modes with branching ratio $\sim \mathcal{O}(10^{-8})$, such as the $B^0 \to K^+K^-$ decay [50], can be accessible at the LHCb experiments now. The branching ratios of the $B_c^* \to \psi\pi$ decays can reach up to $\mathcal{O}(10^{-8})$. In addition, according to the estimation of Ref. [14], the production cross section of the B_c^* meson is about 30 nb at LHC. It is

promisingly expected to have more than 10^{10} B_c^* meson samples, corresponding to hundreds of the $B_c^* \to \psi(1S)\pi$, $\psi(2S)\pi$ decays, per ab^{-1} data accumulated at LHC. The possible background from the $B_c \to \psi\pi$ decays might, in principle, be excluded from the invariant mass of final states. So, even given the detection efficiency, the $B_c^* \to J/\psi\pi$ decay is also measurable, although very challenging, at the future LHC experiments.

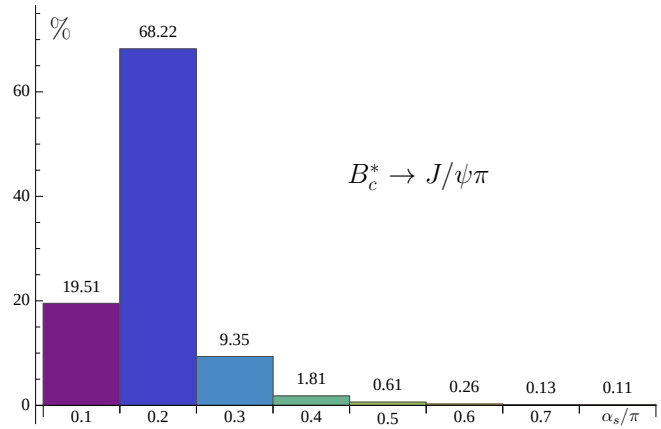

FIG. 3: Contributions to branching ratio $\mathcal{B}r(B_c^* \to J/\psi\pi)$ from different regions of α_s/π (abscissa axis), where the numbers above the histogram denote the percentage of the corresponding contributions.

(3) The spectator quarks in the $B_c^* \to \psi$ and $B_c^* \to \eta_c$ transitions are the heavy charm quark. It is usually assumed that the charm quark in the B_c^* meson and charmonium might be close to on-shell, and the gluons emitted or absorbed by the spectator quarks might be soft. It is natural to question the validity of perturbative calculation and the practicability of pQCD approach. In order to eliminate the doubts, it is necessary to check how many shares come from the perturbative domain. The contributions to branching ratio $\mathcal{B}r(B_c^* \to J/\psi\pi)$ from different α_s/π region are displayed in Fig.3. It is clearly seen that more than 85% (95%) contributions to branching ratio $\mathcal{B}r(B_c^* \to J/\psi\pi)$ come from the $\alpha_s/\pi \leq 0.2$ (0.3) regions, which implies that the perturbative calculation with the pQCD approach is feasible and credible. The small Wilson coefficient C_1 and the small coupling α_s at a higher scale μ will account for the small percentage from the $\alpha_s/\pi \leq 0.1$ region. The tiny share from the $\alpha_s/\pi \geq 0.5$ region is caused by the serious suppression on soft contributions from many factors, such as Sudakov factor, DAs for the B_c^* meson and charmonium. In addition, a preferable convention to choose the scale as the largest one of all virtualities of internal particles [see Eq.(A27) and Eq.(A28)] is employed to ensure the perturbative calculation

with the pQCD approach.

(4) The theoretical predictions have large uncertainties. With the precent predictions on branching ratios of the $B_c^* \to \psi P$, $\eta_c P$ decays, strict constraints on parameters (such as the CKM matrix element $|V_{cb}|$ and decay width $\Gamma_{B_c^*}$) cannot be obtained. A global fit with more observables seems to be necessary. The first uncertainty from the typical scale μ might, in principle, be reduced by the inclusion of higher order corrections to HMEs. The decay amplitudes are closely related with wave functions [see Eq.(4)], and parameters of m_b and m_c have much influence on wave functions used here. The third uncertainty arises mainly from the Wolfenstein parameter A, i.e., $\frac{2\,\delta A}{A} \sim 6.4\%$. And a large uncertainty comes from the indefinitive decay width $\Gamma_{B_c^*}$. The uncertainties from m_b and m_c, the CKM parameters, and $\Gamma_{B_c^*}$ are expected to reduce greatly through either the relative ratio of branching ratios or other observables, such as the polarization fractions $f_{0,\parallel,\perp} = \frac{|\mathcal{M}_{0,\parallel,\perp}|^2}{|\mathcal{M}_0|^2+|\mathcal{M}_\parallel|^2+|\mathcal{M}_\perp|^2}$. Our studies show that the dominant contributions come from the factorizable topologies. There are large cancellations between the nonfactorizable contributions. Thus the effects from possible new physics should be imperceptible. The more dedicated studies are deserved in the future.

IV. SUMMARY

It is expected that there would be a huge amount of the B_c^* meson data samples at the LHC, and there would be a realistic possibility to search for the B_c^* meson weak decays in the future. In this paper, the nonleptonic $B_c^* \to \psi(1S,2S)P$, $\eta_c(1S,2S)P$ decays are studied first with a phenomenological pQCD approach, in order to offer a ready reference for the future experimental analysis. It is found that branching ratio for the $B_c^* \to J/\psi\pi$ decay is about $\sim \mathcal{O}(10^{-8})$, which could be accessible at the future experiments.

Appendix A: Amplitude building blocks for the $B_c^* \to \psi P$, $\eta_c P$ decays

$$\begin{aligned}\mathcal{A}_{a,P} &= 2\,m_1\,(\epsilon_1\cdot p_2)\int_0^1 dx_1\int_0^1 dx_2\int_0^\infty b_1 db_1\int_0^\infty b_2 db_2\, H_f(\alpha,\beta_a,b_1,b_2)\,\alpha_s(t_a)\\ &\times\; E_f(t_a)\,a_1(t_a)\,\phi^v_{B_c^*}(x_1)\left\{\phi^a_{\eta_c}(x_2)\,(m_1^2\,\bar{x}_2+m_3^2\,x_2)+\phi^p_{\eta_c}(x_2)\,m_2\,m_b\right\},\end{aligned} \tag{A1}$$

$$\mathcal{A}_{a,L} = \int_0^1 dx_1 \int_0^1 dx_2 \int_0^\infty b_1 db_1 \int_0^\infty b_2 db_2\, H_f(\alpha,\beta_a,b_1,b_2)\,\alpha_s(t_a)\,E_f(t_a) \times a_1(t_a)\,\phi^v_{B_c^*}(x_1)\left\{\phi^v_\psi(x_2)\,(m_1^2\,s\,\bar{x}_2 + m_3^2\,t\,x_2) + \phi^t_\psi(x_2)\,m_2\,m_b\,u\right\}, \tag{A2}$$

$$\mathcal{A}_{a,N} = m_1 \int_0^1 dx_1 \int_0^1 dx_2 \int_0^\infty b_1 db_1 \int_0^\infty b_2 db_2\, H_f(\alpha,\beta_a,b_1,b_2)\,\alpha_s(t_a) \times E_f(t_a)\,a_1(t_a)\,\phi^V_{B_c^*}(x_1)\left\{\phi^V_\psi(x_2)\,m_2\,(u - s\,x_2) + \phi^T_\psi(x_2)\,m_b\,s\right\}, \tag{A3}$$

$$\mathcal{A}_{a,T} = 2\,m_1 \int_0^1 dx_1 \int_0^1 dx_2 \int_0^\infty b_1 db_1 \int_0^\infty b_2 db_2\, H_f(\alpha,\beta_a,b_1,b_2)\,\alpha_s(t_a) \times E_f(t_a)\,a_1(t_a)\,\phi^V_{B_c^*}(x_1)\left\{\phi^V_\psi(x_2)\,m_2\,\bar{x}_2 + \phi^T_\psi(x_2)\,m_b\right\}, \tag{A4}$$

$$\mathcal{A}_{b,P} = 2\,m_1\,(\epsilon_1\cdot p_2) \int_0^1 dx_1 \int_0^1 dx_2 \int_0^\infty b_1 db_1 \int_0^\infty b_2 db_2\, H_f(\alpha,\beta_b,b_2,b_1) \times \alpha_s(t_b)\,E_f(t_b)\left\{\phi^t_{B_c^*}(x_1)\left[\phi^p_{\eta_c}(x_2)\,2\,m_1\,m_2\,\bar{x}_1 - \phi^a_{\eta_c}(x_2)\,m_1\,m_c\right] + \phi^v_{B_c^*}(x_1)\left[\phi^p_{\eta_c}(x_2)\,2\,m_2\,m_c - \phi^a_{\eta_c}(x_2)\,(m_2^2\,\bar{x}_1 + m_3^2\,x_1)\right]\right\} a_1(t_b), \tag{A5}$$

$$\mathcal{A}_{b,L} = \int_0^1 dx_1 \int_0^1 dx_2 \int_0^\infty b_1 db_1 \int_0^\infty b_2 db_2\, H_f(\alpha,\beta_b,b_2,b_1)\,\alpha_s(t_b)\,E_f(t_b) \times a_1(t_b)\,\phi^v_\psi(x_2)\left\{\phi^v_{B_c^*}(x_1)\,(m_2^2\,u\,\bar{x}_1 - m_3^2\,t\,x_1) + \phi^t_{B_c^*}(x_1)\,m_1\,m_c\,s\right\}, \tag{A6}$$

$$\mathcal{A}_{b,N} = m_2 \int_0^1 dx_1 \int_0^1 dx_2 \int_0^\infty b_1 db_1 \int_0^\infty b_2 db_2\, H_f(\alpha,\beta_b,b_2,b_1)\,E_f(t_b) \times \alpha_s(t_b)\,a_1(t_b)\,\phi^V_\psi(x_2)\left\{\phi^V_{B_c^*}(x_1)\,m_1\,(s - u\,x_1) + \phi^T_{B_c^*}(x_1)\,m_c\,u\right\}, \tag{A7}$$

$$\mathcal{A}_{b,T} = 2\,m_2 \int_0^1 dx_1 \int_0^1 dx_2 \int_0^\infty b_1 db_1 \int_0^\infty b_2 db_2\, H_f(\alpha,\beta_b,b_2,b_1)\,\alpha_s(t_b) \times E_f(t_b)\,a_1(t_b)\,\phi^V_\psi(x_2)\left\{\phi^V_{B_c^*}(x_1)\,m_1\,\bar{x}_1 + \phi^T_{B_c^*}(x_1)\,m_c\right\}, \tag{A8}$$

$$\mathcal{A}_{c,P} = \frac{2\,m_1\,(\epsilon_1\cdot p_2)}{N_c} \int_0^1 dx_1 \int_0^1 dx_2 \int_0^1 dx_3 \int_0^\infty db_1 \int_0^\infty b_2 db_2 \int_0^\infty b_3 db_3 \times H_n(\alpha,\beta_c,b_1,b_2,b_3)\,\alpha_s(t_c)\left\{\phi^v_{B_c^*}(x_1)\,\phi^a_{\eta_c}(x_2)\,s\,(x_2 - \bar{x}_3) + \phi^t_{B_c^*}(x_1)\,\phi^p_{\eta_c}(x_2)\,m_1\,m_2\,(x_1 - x_2)\right\}\phi^a_P(x_3)\,E_n(t_c)\,C_2(t_c), \tag{A9}$$

$$\mathcal{A}_{c,L} = \frac{1}{N_c}\int_0^1 dx_1\int_0^1 dx_2\int_0^1 dx_3\int_0^\infty db_1\int_0^\infty b_2 db_2\int_0^\infty b_3 db_3\,\alpha_s(t_c)\,E_n(t_c)$$
$$\times\ H_n(\alpha,\beta_c,b_1,b_2,b_3)\,\phi_P^a(x_3)\Big\{\phi_{B_c^*}^v(x_1)\,\phi_\psi^v(x_2)\,4\,m_1^2\,p^2\,(x_2-\bar{x}_3)$$
$$+\phi_{B_c^*}^t(x_1)\,\phi_\psi^t(x_2)\,m_1\,m_2\,(u\,x_1-s\,x_2-2\,m_3^2\,\bar{x}_3)\Big\}\,C_2(t_c), \tag{A10}$$

$$\mathcal{A}_{c,N} = \frac{1}{N_c}\int_0^1 dx_1\int_0^1 dx_2\int_0^1 dx_3\int_0^\infty db_1\int_0^\infty b_2 db_2\int_0^\infty b_3 db_3\,H_n(\alpha,\beta_c,b_1,b_2,b_3)\,\alpha_s(t_c)$$
$$\times\ E_n(t_c)\,C_2(t_c)\,\phi_{B_c^*}^T(x_1)\,\phi_\psi^T(x_2)\,\phi_P^a(x_3)\Big\{m_1^2\,s\,(x_1-\bar{x}_3)+m_2^2\,u\,(\bar{x}_3-x_2)\Big\}, \tag{A11}$$

$$\mathcal{A}_{c,T} = \frac{2}{N_c}\int_0^1 dx_1\int_0^1 dx_2\int_0^1 dx_3\int_0^\infty db_1\int_0^\infty b_2 db_2\int_0^\infty b_3 db_3\,H_n(\alpha,\beta_c,b_1,b_2,b_3)\,\alpha_s(t_c)$$
$$\times\ E_n(t_c)\,C_2(t_c)\,\phi_{B_c^*}^T(x_1)\,\phi_\psi^T(x_2)\,\phi_P^a(x_3)\Big\{m_1^2\,(x_1-\bar{x}_3)+m_2^2\,(\bar{x}_3-x_2)\Big\}, \tag{A12}$$

$$\mathcal{A}_{d,P} = \frac{2\,m_1\,(\epsilon_1\cdot p_2)}{N_c}\int_0^1 dx_1\int_0^1 dx_2\int_0^1 dx_3\int_0^\infty db_1\int_0^\infty b_2 db_2\int_0^\infty b_3 db_3$$
$$\times\ H_n(\alpha,\beta_d,b_1,b_2,b_3)\,E_n(t_d)\Big\{\phi_{B_c^*}^t(x_1)\,\phi_{\eta_c}^p(x_2)\,m_1\,m_2\,(x_1-x_2)$$
$$+\ \phi_{B_c^*}^v(x_1)\,\phi_{\eta_c}^a(x_2)\,(2\,m_2^2\,x_2+s\,x_3-t\,x_1)\Big\}\,\alpha_s(t_d)\,C_2(t_d)\,\phi_P^a(x_3), \tag{A13}$$

$$\mathcal{A}_{d,L} = \frac{1}{N_c}\int_0^1 dx_1\int_0^1 dx_2\int_0^1 dx_3\int_0^\infty db_1\int_0^\infty b_2 db_2\int_0^\infty b_3 db_3\,\alpha_s(t_d)\,E_n(t_d)$$
$$\times\ H_n(\alpha,\beta_d,b_1,b_2,b_3)\,\phi_P^a(x_3)\Big\{\phi_{B_c^*}^v(x_1)\,\phi_\psi^v(x_2)\,4\,m_1^2\,p^2\,(x_3-x_1)$$
$$-\phi_{B_c^*}^t(x_1)\,\phi_\psi^t(x_2)\,m_1\,m_2\,(u\,x_1-s\,x_2-2\,m_3^2\,x_3)\Big\}\,C_2(t_d), \tag{A14}$$

$$\mathcal{A}_{d,N} = \frac{1}{N_c}\int_0^1 dx_1\int_0^1 dx_2\int_0^1 dx_3\int_0^\infty db_1\int_0^\infty b_2 db_2\int_0^\infty b_3 db_3\,H_n(\alpha,\beta_d,b_1,b_2,b_3)\,\alpha_s(t_d)$$
$$\times\ E_n(t_d)\,C_2(t_d)\,\phi_{B_c^*}^T(x_1)\,\phi_\psi^T(x_2)\,\phi_P^a(x_3)\Big\{m_1^2\,s\,(x_3-x_1)+m_2^2\,u\,(x_2-x_3)\Big\}, \tag{A15}$$

$$\mathcal{A}_{d,T} = \frac{2}{N_c}\int_0^1 dx_1\int_0^1 dx_2\int_0^1 dx_3\int_0^\infty db_1\int_0^\infty b_2 db_2\int_0^\infty b_3 db_3\,H_n(\alpha,\beta_d,b_1,b_2,b_3)\,\alpha_s(t_d)$$
$$\times\ E_n(t_d)\,C_2(t_d)\,\phi_{B_c^*}^T(x_1)\,\phi_\psi^T(x_2)\,\phi_P^a(x_3)\Big\{m_1^2\,(x_3-x_1)+m_2^2\,(x_2-x_3)\Big\}, \tag{A16}$$

where the subscript i of $\mathcal{A}_{i,j}$ corresponds to the indices of Fig.2; the subscript j refers to possible helicity amplitudes.

The function $H_{f,n}$ and Sudakov factor $E_{f,n}$ are defined as

$$H_f(\alpha,\beta,b_i,b_j) \;=\; K_0(b_i\sqrt{-\alpha})\left\{\theta(b_i-b_j)K_0(b_i\sqrt{-\beta})\,I_0(b_j\sqrt{-\beta})+(b_i\leftrightarrow b_j)\right\}, \tag{A17}$$

$$\begin{aligned} H_n(\alpha,\beta,b_1,b_2,b_3) \;=\; & \left\{\theta(-\beta)\,K_0(b_3\sqrt{-\beta})+\frac{\pi}{2}\,\theta(\beta)\left[i\,J_0(b_3\sqrt{\beta})-Y_0(b_3\sqrt{\beta})\right]\right\} \\ & \times\left\{\theta(b_2-b_3)\,K_0(b_2\sqrt{-\alpha})\,I_0(b_3\sqrt{-\alpha})+(b_2\leftrightarrow b_3)\right\}\delta(b_1-b_2), \end{aligned} \tag{A18}$$

$$E_f(t) \;=\; \exp\{-S_{B_c^*}(t)-S_{\psi,\eta_c}(t)\}, \tag{A19}$$

$$E_n(t) \;=\; \exp\{-S_{B_c^*}(t)-S_{\psi,\eta_c}(t)-S_P(t)\}, \tag{A20}$$

$$S_i(t) \;=\; s(x_i,b_i,p_i^+)+s(\bar{x}_i,b_i,p_i^+)+2\int_{1/b_i}^{t}\frac{d\mu}{\mu}\gamma_q, \tag{A21}$$

where I_0, J_0, K_0 and Y_0 are Bessel functions; $\gamma_q=-\alpha_s/\pi$ is the quark anomalous dimension; the expression of $s(x,b,Q)$ can be found in of Ref.[15]; α and β_i are virtualities of gluon and quarks. The definitions of the particle virtuality and typical scale t_i are given as follows.

$$\alpha \;=\; x_1^2\,m_1^2+x_2^2\,m_2^2-x_1\,x_2\,t, \tag{A22}$$

$$\beta_a \;=\; m_1^2+x_2^2\,m_2^2-x_2\,t-m_b^2, \tag{A23}$$

$$\beta_b \;=\; m_2^2+x_1^2\,m_1^2-x_1\,t-m_c^2, \tag{A24}$$

$$\beta_c \;=\; \alpha+\bar{x}_3^2\,m_3^2-x_1\,\bar{x}_3\,u+x_2\,\bar{x}_3\,s, \tag{A25}$$

$$\beta_d \;=\; \alpha+x_3^2\,m_3^2-x_1\,x_3\,u+x_2\,x_3\,s, \tag{A26}$$

$$t_{a,b} \;=\; \max\{\sqrt{-\alpha},\sqrt{|\beta_{a,b}|},1/b_1,1/b_2\}, \tag{A27}$$

$$t_{c,d} \;=\; \max\{\sqrt{-\alpha},\sqrt{|\beta_{c,d}|},1/b_2,1/b_3\}. \tag{A28}$$

[1] R. Dowdall *et al.* (HPQCD Collaboration), Phys. Rev. D 86, 094510 (2012).

[2] V. Šimonis, Eur. Phys. J. A 52, 90 (2016).

[3] N. Brambilla *et al.* (Quarkonium Working Group), arXiv:hep-ph/0412158, and references therein.

[4] M. Lusignoli, M. Masetti, Z. Phys. C 51, 549 (1991).

[5] C. Chang, Y. Chen, Phys. Rev. D 49, 3399 (1994).

[6] S. Gershtein *et al.*, Phys. Usp. 38, 1 (1995).

[7] J. Sun, D. Du, Y. Yang, Eur. Phys. J. C 60, 107 (2009).

[8] J. Sun *et al.*, Phys. Rev. D 77, 074013 (2008).

[9] J. Sun *et al.*, Phys. Rev. D 89, 114019 (2014).

[10] C. Patrignani *et al.* (Particle Data Group), Chin. Phys. C 40, 100001 (2016).

[11] C. Chang *et al.*, Phys. Lett. B 364, 78 (1995).

[12] C. Chang, Y. Chen, R. Oakes, Phys. Rev. D 54, 4344 (1996).

[13] C. Chang, X. Wu, Eur. Phys. J. C 38, 267 (2004).

[14] C. Chang *et al.*, Phys. Rev. D 72, 114009 (2005).

[15] H. Li, Phys. Rev. D 52, 3958 (1995).

[16] C. Chang, H. Li, Phys. Rev. D 55, 5577 (1997).

[17] T. Yeh, H. Li, Phys. Rev. D 56, 1615 (1997).

[18] V. Abazov *et al.* (D0 Collaboration), Phys. Rev. Lett. 101, 012001 (2008).

[19] T. Aaltonen *et al.* (CDF Collaboration), Phys. Rev. D 87, 011101 (2013).

[20] V. Khachatryan *et al.* (CMS Collaboration), JHEP, 1501, 063 (2015).

[21] R. Aaij *et al.* (LHCb Collaboration), Phys. Rev. D 90, 032009 (2014).

[22] R. Aaij *et al.* (LHCb Collaboration), JHEP, 1609, 153 (2016).

[23] R. Aaij *et al.* (LHCb Collaboration), Phys. Rev. D 92, 072007 (2015).

[24] G. Buchalla, A. Buras, M. Lautenbacher, Rev. Mod. Phys. 68, 1125, (1996).

[25] G. Lepage, S. Brodsky, Phys. Rev. D 22, 2157 (1980).

[26] M. Beneke *et al.*, Phys. Rev. Lett. 83, 1914 (1999).

[27] M. Beneke *et al.*, Nucl. Phys. B 591, 313 (2000).

[28] M. Beneke *et al.*, Nucl. Phys. B 606, 245 (2001).

[29] T. Kurimoto, H. Li, A. Sanda, Phys. Rev. D 65, 014007 (2001).

[30] P. Ball, V. Braun, A. Lenz, JHEP, 0605, 004 (2006).

[31] Y. Yang *et al.*, Phys. Lett. B 751, 171 (2015).

[32] J. Sun *et al.*, Phys. Lett. B 752, 322 (2016).

[33] Y. Yang *et al.*, Int. J. Mod. Phys. A 31, 1650146 (2016).

[34] J. Sun *et al.*, Nucl. Phys. B 911, 890 (2016).

[35] G. Lepage *et al.*, Phys. Rev. D 46, 4052 (1992).

[36] G. Bodwin, E. Braaten, G. Lepage, Phys. Rev. D 51, 1125 (1995).

[37] N. Brambilla *et al.*, Rev. Mod. Phys. 77, 1423 (2005).

[38] B. Colquhoun *et al.* (HPQCD Collaboration), Phys. Rev. D 91, 114509 (2015).

[39] M. Gómez-Rocha, T. Hilger, A. Krassnigg, Phys. Rev. D 93, 074010 (2016).

[40] J. Lansberg, T. Pham, Phys. Rev. D 74, 034001 (2006).

[41] N. Barik, P. Dash, Phys. Rev. D 49 299 (1994).

[42] E. Eichten, C. Quigg, Phys. Rev. D 49, 5845 (1994).

[43] S. Gershtein *et al.*, Phys. Rev. D 51, 3613 (1995).

[44] L. Fulcher, Phys. Rev. D 60, 074006 (1999).

[45] D. Ebert, R. Faustov, V. Galkin, Phys. Rev. D 67, 014027 (2003).

[46] S. Godfrey, Phys. Rev. D 70, 054017 (2004).

[47] S. Jena, P. Panda, T. Tripathy, Nucl. Phys. A 699, 649 (2002).

[48] T. Lahde, Nucl. Phys. A 714, 183 (2003).

[49] H. Ciftci, H. Koru, Mod. Phys. Lett. A 16, 1785 (2001).

[50] R. Aaij *et al.* (LHCb Collaboration), Phys. Rev. Lett. 118, 081801 (2017).